

# Molecular gas in spiral galaxies

F. Casoli<sup>1</sup>, S. Sauty<sup>1</sup>, M. Gerin<sup>2,1</sup>, A. Boselli<sup>3</sup>, P. Fouqué<sup>4</sup>, J. Braine<sup>5</sup>, G. Gavazzi<sup>6</sup>, J. Lequeux<sup>1</sup>, and J. Dickey<sup>7</sup>

<sup>1</sup> DEMIRM, Observatoire de Paris, 61 Av. de l'Observatoire, F-75014 Paris, France; and URA336 du CNRS

<sup>2</sup> Radioastronomie Millimétrique, ENS, 24 Rue Lhomond, F-75231 Paris cedex 05, France; and URA336 du CNRS

<sup>3</sup> Laboratoire d'Astronomie Spatiale, Traverse du Siphon, F-13376 Marseille Cedex 12, France

<sup>4</sup> ESO, Alonso de Cordova 3107, Vitacura, Casilla 19001, Santiago 19, Chile

<sup>5</sup> Observatoire de Bordeaux, URA 352, CNRS/INSU, BP 89, F-33270 Floirac, France

<sup>6</sup> Osservatorio di Brera, via Brera 28, I-20121 Milano, Italy

<sup>7</sup> Astronomy Department, University of Minnesota, 116 Church Street SE, Minneapolis, MN 55455, USA

Received 12 December 1996 / Accepted 3 November 1997

**Abstract.** The molecular hydrogen content of a galaxy is a key parameter for its activity and future evolution. Its variations with basic properties such as size, mass, morphological type, and environment, the ratio of molecular to atomic gas masses, should provide us with a better view of galaxy evolution. Such studies have been done in the past by Sage (1993a) or the FCRAO group (e.g. Young & Knezek 1989), and have led to controversial results, for example about the  $M_{\text{H}_2}/M_{\text{HI}}$  ratio. While Sage (1993a), using a distance-limited sample of 65 galaxies and the CO(1–0) line emission as a tracer of the  $\text{H}_2$  mass, finds that most galaxies have  $M_{\text{H}_2}/M_{\text{HI}}$  lower than 1, Young & Knezek (1989) and Young et al. (1995), from a different sample of 178 objects, claim equal amounts of gas in the molecular and atomic phase.

Here we again tackle this problem, by gathering a much larger sample of 582 objects, not only from the literature but also from several CO(1–0) surveys that we have completed and which are largely unpublished. Our sample is clearly not complete and contains a large number of cluster galaxies as well as many more massive objects than a distance-limited sample. Contrary to previous analyses, we have taken into account the non-detections by using the survival analysis method. Our sample includes 105 isolated galaxies, observed by us, that we use as a reference sample in order to determine whether cluster galaxies are CO-deficient.

We find that the ratio of  $\text{H}_2$  and HI masses is on the average lower than 1, with  $\langle \log(M_{\text{H}_2}/M_{\text{HI}}) \rangle = \log(0.20) \pm 0.04$  (median =  $\log(0.27) \pm 0.04$ ). For spirals with types Sa to Sc, we have slightly higher values:  $\log(0.28)$  and  $\log(0.34)$  respectively. The actual  $\text{H}_2$  masses and  $M_{\text{H}_2}/M_{\text{HI}}$  ratios could be lower than given above if, as suggested by recent  $\gamma$ -ray and 1.3 mm continuum data, the conversion factor between CO(1–0) emissivities and  $\text{H}_2$  masses for large spiral galaxies is lower than the value adopted here ( $X=2.3 \cdot 10^{20} \text{ cm}^{-2}/(\text{K kms}^{-1})$ ).

The molecular to atomic gas ratio shows a constant value from Sa to Sbc's, and a factor of 10 decrease for late-types, beginning at Sc's. This effect can be attributed to the low CO emission of late-type, low-mass galaxies; we find no such decrease for objects with a dynamical mass larger than  $10^{11} M_{\odot}$ . These high-mass objects actually show an increase of their normalized atomic and molecular gas content towards late-types, while for low-mass objects, this is seen on HI only.

Several authors have tried to search for galaxies deficient in  $\text{H}_2$  in the core of clusters such as Virgo or Coma, but these studies were hampered by the lack of a suitable reference sample (Kenney & Young 1989, Casoli et al. 1991, Horellou et al. 1995b). Using isolated galaxies and galaxies in the outer regions of clusters as a reference sample, we give a predictor for the normalized  $\text{H}_2$  mass of a galaxy  $M_{\text{H}_2}^i/D_{25}^2$ , which depends upon its normalized far-infrared emission  $L_{\text{FIR}}/D_{25}^2$  and its morphological type. This predictor allows us to define a “CO deficiency factor”, CODEF, analogous to what has been defined for the HI emission. We find that there is no significant CO deficiency of galaxies in the cores of rich clusters.

**Key words:** galaxies: evolution – galaxies: spiral – ISM: molecules – galaxies: statistics

---

## 1. The phases of the ISM in disc galaxies

The cold neutral interstellar medium of galaxies is found under two phases: atomic and molecular, but it is probably only in the molecular phase that stars are formed. Knowing the variations of the  $\text{H}_2$  content and of the  $M_{\text{H}_2}/M_{\text{HI}}$  ratio with basic properties of a galaxy such as its size and morphological type, and with its environment, might then help to understand the star formation process in galaxies and its time evolution. The most widely used tracer of the molecular phase is the CO(1–0) line emission at

2.6 mm. The reliability of this indicator is a matter of debate for galactic observations, and all the more so for extragalactic ones (for a recent discussion see Boselli et al. 1995a and Lequeux 1996). There have been several major surveys of galaxies in this line, such as the FCRAO extragalactic survey (Young et al 1995), with 300 objects surveyed, which are mostly selected for their brightness in the visible and far-infrared, and the survey of all galaxies nearer than 10 Mpc undertaken by Sage (1993a, b; hereafter S93). There are a number of points left unclear by these studies. For example, the analysis of part of the data in the FCRAO extragalactic survey indicates an almost equal amount of mass in both phases of the interstellar medium (Young & Knezek 1989, hereafter YK); on the other hand the study by Sage suggests a low fraction of gas in molecular form. These studies evidence a strong decrease of the  $H_2/HI$  ratio when going from early to late types: it is about a factor of 20 for YK, but 10 for S93. Another point is that of the existence of CO-deficient galaxies in the core of clusters; Kenney & Young (1989) have found no evidence for CO-deficient galaxies in the Virgo; similar conclusions were reached for the Coma supercluster by Casoli et al. (1991) and for the Fornax cluster by Horellou et al. (1995b), but all these studies were hampered by the absence of a suitable comparison sample of isolated galaxies.

We have thus tried to study the CO(1–0) emission and  $H_2$  molecular content of disc galaxies in a more systematic way, and gathered a large database of CO(1–0) observations of galaxies, extracted from several surveys completed by our group and from the literature. Using this sample, we study the variation of the CO(1–0) emission (and presumably of the molecular hydrogen mass) and of the molecular gas fraction with basic properties of the galaxy: size, mass and morphological type, and finally the cluster environment.

## 2. The sample

To build our sample, we have gathered CO(1–0) data from various sources. From the literature we have obtained data for 305 objects: we have used the FCRAO extragalactic survey (Young et al. 1989, 1995) and the survey of nearby galaxies by Sage (1993 a, b). The remaining 277 sources have been observed by us, in the course of several surveys that we have made using the NRAO 12m, SEST 15m, and Onsala 20m telescopes: Fornax cluster (Horellou et al. 1995b), Coma supercluster region (Casoli et al. 1991, 1996, Boselli et al. 1994, 1995b), ComaI group (Gerin & Casoli 1994), IRAS-selected objects (Andreani et al. 1995), ring galaxies (Horellou et al. 1995a) and isolated galaxies from the Karachenseva (1973) catalog (Sauty et al. 1997). Some galaxies are in common between the FCRAO and Sage samples; in this case we have kept Sage’s observations because they have been mainly obtained with the NRAO 12m, as were our own data on the Coma supercluster and isolated galaxies. This ensures some degree of consistency between the data. Some of these galaxies have been observed at their center only or along their major axis, in which case the observed emission has been extrapolated to get an estimate of the total mass (see Young et al. 1995, Sauty et al. 1997 for details).

The sample comprises 582 galaxies in total. Contrary to the work done by S93, our sample is not distance-limited, and contains many more massive objects. These galaxies are found in a variety of environments: isolated objects, small groups, as well many galaxies in clusters: Coma supercluster, Fornax and Virgo. This sample may thus be not truly representative of genuine “field” galaxies. Among these cluster members, there are some severely HI-deficient objects. If we want to study the molecular to atomic gas ratio, it is clear that these objects have to be excluded from the analysis. We will then exclude all *cluster* galaxies with an HI-deficiency (as defined by Giovanelli & Haynes 1985) larger than 0.5. The excluded galaxies thus have an HI content three times lower than what could be expected from their optical area and morphological type. The remaining “HI-normal” sample amounts to 529 objects. The HI-deficient objects will be considered again in Sect. 4, where we will discuss the problem of the CO(1–0) emission of galaxies in clusters.

$H_2$  masses have been computed using a conversion factor  $N(H_2)/I(CO)=X=2.3 \cdot 10^{20} \text{ cm}^{-2}/(\text{K kms}^{-1})$  (Strong et al. 1988). As a reminder that these are only “indicative”  $H_2$  masses, we will denote them as  $M_{H_2}^i$ . Blue and far-infrared luminosities were computed as in Casoli et al. (1996), and we have used  $H_0 = 75 \text{ km s}^{-1}/\text{Mpc}$ . In the Coma supercluster, galaxy distances were computed according to Casoli et al. (1996). Data from the literature have been scaled to our values of  $X$  and  $H_0$ . HI masses, morphological types, optical diameters and magnitudes have been mainly extracted from the LEDA database (Paris-Lyon-Meudon Observatories) but most of these data for the Coma supercluster galaxies come from recent CCD observations (see Casoli et al. 1996). IRAS flux densities have been obtained from the NED database at IPAC.

There are 137 non-detections in the CO(1–0) line (125 for the HI-normal subsample). In order to take into account the information contained in these non-detections, we have used the technique known as survival analysis (Isobe et al. 1986).

## 3. Variations of $M_{H_2}^i$ and $M_{HI}$ with morphological types and dynamical masses

### 3.1. Gas content and morphological type

In this Section, we will examine the variations of the atomic and molecular gas contents with the morphological type of the galaxies. The trends that we find for the atomic gas masses are already known, but we will show them for comparison purposes. The first step is normalization. Indeed, because of the well-known tendency that big galaxies have more of everything, the gas masses need to be normalized to some quantity related to the galaxy “size”. Several normalizations can be thought of: total blue luminosity  $L_B$ , optical area (square of the blue diameter at the 25-th magnitude per arcsec<sup>2</sup>,  $D_{25}^2$ ), H-band luminosity  $L_H$ , or dynamical mass  $M_{\text{dyn}}$ . We will use here mainly the normalization by the optical area  $D_{25}^2$  which has been shown to be the best one for the HI content, since little residual variation is then left. We will see that things are a little more complicated for the molecular phase (Sect. 4). Note that  $M_{H_2}^i/D_{25}^2$  and

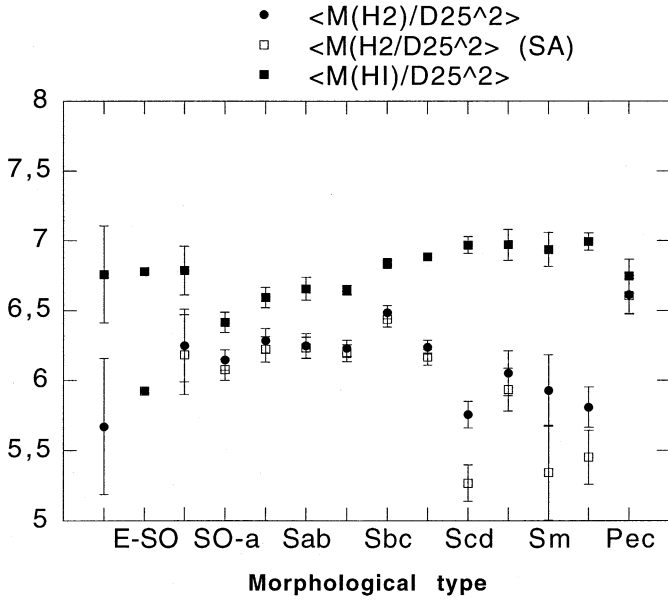


**Fig. 1.** Variation of the gas contents for the 529 galaxies in the HI-normal sample, normalized to the optical area, along the morphological type sequence. Pec indicates very perturbed or interacting objects such as ring galaxies. Dots show mean values of  $M_{\text{H}_2}^i/D_{25}^2$  with upper limits treated as detections, while the errorbars give the error on the mean. Open squares give the mean values of  $M_{\text{H}_2}^i/D_{25}^2$  computed using survival analysis. For the HI phase, since there are 8 non-detections only in this “HI-normal” sample, the values using survival analysis are not shown.

$M_{\text{HI}}/D_{25}^2$  have units of gas surface densities,  $\sigma_{\text{H}_2}$  and  $\sigma_{\text{HI}}$ , but do not correspond to physical gas surface densities, because of the high degree of inhomogeneity of the molecular phase and of the difference between the gas and optical scale lengths (see Casoli et al. 1996). Normalizing by  $L_B$  gives essentially the same results. The H-band luminosity would be a good measure of the total stellar mass of the galaxy, but there are not enough data in this band for our purpose. We will then use  $M_{\text{dyn}}$ , an estimate of the dynamical mass inside the optical radius, computed from:

$$M_{\text{dyn}} = (D_{25}/2)(\Delta V)^2 / (G \sin^2 i) (M_{\odot}),$$

where  $\Delta V$  is the HI linewidth at the 20 percent level,  $i$  is the galaxy inclination to the plane of the sky, and  $G$  is the gravitational constant ( $1/232$  if masses are given in solar masses, the velocity width is in km/s and the optical radius  $D_{25}/2$  in pc).  $M_{\text{dyn}}$  has no sense for spheroidal systems, and it was not computed for E’s and E/SO’s. It was not computed either for galaxies with an inclination to the line of sight smaller than  $30^\circ$ .

Table 1 gathers the mean and median values of  $M_{\text{H}_2}^i/D_{25}^2$  and  $M_{\text{HI}}/D_{25}^2$  for each morphological type computed first by treating upper limits as detections, and second by the survival analysis method. Fig. 1 presents the variation of  $M_{\text{H}_2}^i/D_{25}^2$  and  $M_{\text{HI}}/D_{25}^2$  with morphological type for the HI-normal sample. It is clear that, on the average, there is more HI than H<sub>2</sub> in these galaxies, except for Pec galaxies. This is at variance with YK, but in good agreement with S93.

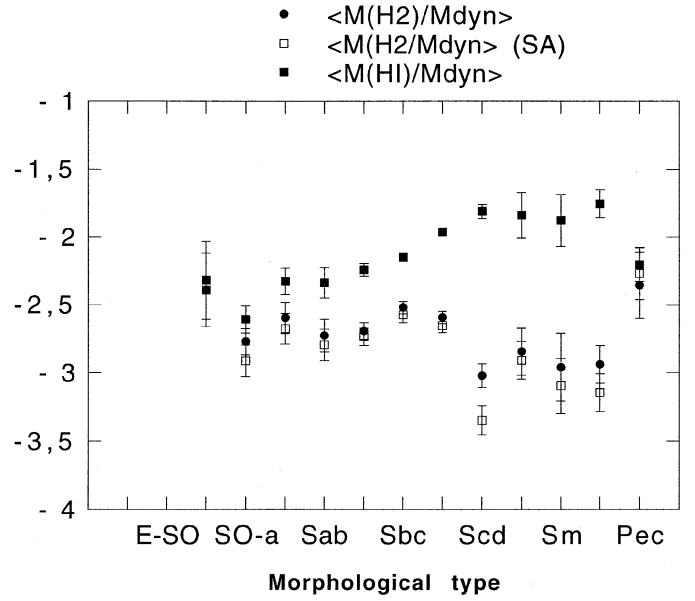


**Fig. 2.** Variation of the gas contents, normalized to the dynamical mass, along the morphological type sequence. No values are given for morphological types E and E/SO, since we have no meaningful estimate of the dynamical mass. Dots show mean values of  $M_{\text{H}_2}^i/M_{\text{dyn}}$  with upper limits treated as detections, while the errorbars give the error on the mean. Open squares give the mean values of  $M_{\text{H}_2}^i/M_{\text{dyn}}$  computed using survival analysis. For the HI phase, since there are 8 non-detections only in this “HI-normal” sample, the values using survival analysis are not shown.

This sample follows the known trend of increasing  $M_{\text{HI}}/D_{25}^2$  and decreasing  $M_{\text{H}_2}^i/D_{25}^2$  for late-type galaxies (Haynes & Giovanelli 1984, Roberts & Haynes 1994). However, while the increase for  $M_{\text{HI}}/D_{25}^2$  is consistent with previous studies (HG84), the effect for the molecular gas is milder than what has been found by YK and more in agreement with S93. The data are actually consistent with a constant value of  $M_{\text{H}_2}^i/D_{25}^2$  for Sa to Sc, that is, for “classical” spirals, and another lower value from Scd to Irr. With the optical area normalization, classical spirals have then about 6 times more H<sub>2</sub> (CO emission) than late-types, and 1.6 times less HI. These numbers have been obtained using survival analysis and would be lower if we treat upper limits as detections, since most of the non-detections are found among late-type spirals. As for the total gas content  $M_{\text{gas}}/D_{25}^2$  (not shown for the clarity of the figure) it increases for late-types, which is not surprising given that most of the gas is found in the atomic phase.

Fig. 2 shows the variations of the gas contents normalized to the dynamical masses. The observed trends are rather similar to what is found with the surface densities, consistent with two values of the normalized gas content, one for the classical spirals and another one for the late-type objects. With this normalization, “classical” spirals have about four times more H<sub>2</sub> (CO emission) than late-types (using survival analysis), and also about twice less HI. These figures are different from what has been found with the optical area normalization, which is not

**Table 1.** Mean values of the gas masses normalized to the optical area,  $\log(M_{\text{H}_2}^i/D_{25}^2)$  and  $\log(M_{\text{HI}}/D_{25}^2)$  ( $M_{\odot}/kpc^2$ ), in the HI-normal sample. Some values could not be computed because there was too few data. Two values are given for the mean: the first one is computed by considering upper limits as detections, the second one, with the subscript SA, was computed using survival analysis. Medians were also computed using survival analysis. N and  $N_d$  are respectively the number of observed and detected objects in each morphological type. Since in this HI-normal sample there are only 8 galaxies undetected in HI, the values given for HI are computed without survival analysis.

T	$H_2$							HI				
	N/ $N_d$	$\langle \rangle$	s.e.	$\langle \rangle_{SA}$	s.e.	$med_{SA}$	s.e.	N	$\langle \rangle$	s.e.	med	s.e.
E	3/3	5.672	.486					3	6.759	.346	6.573	.471
E-S0	1/1	5.924						1	6.780		6.780	
SO	9/7	6.249	.260	6.184	.286	6.231	.421	9	6.786	.174	6.730	.301
SO-a	32/20	6.148	.072	6.078	.077	5.997	.122	32	6.416	.074	6.424	.030
Sa	39/28	6.286	.088	6.223	.092	6.190	.129	39	6.594	.074	6.620	.032
Sab	36/24	6.249	.088	6.233	.076	6.129	.038	36	6.657	.081	6.663	.111
Sb	77/68	6.230	.058	6.195	.060	6.278	.135	77	6.646	.035	6.660	.019
Sbc	101/88	6.487	.047	6.438	.055	6.467	.083	101	6.838	.037	6.843	.075
Sc	133/114	6.238	.049	6.168	.056	6.234	.045	133	6.885	.024	6.852	.023
Scd	27/11	5.758	.094	5.268	.130	4.740		27	6.969	.060	6.927	.069
Sd	14/9	6.051	.160	5.935	.152	5.709	.260	14	6.970	.111	6.988	.047
Sm	14/6	5.927	.254	5.344	.338	4.477		14	6.936	.122	7.064	.100
Irr	21/11	5.810	.143	5.452	.192	5.464	.467	21	6.993	.062	7.064	.087
Pec	16/13	6.613	.138	6.603	.124	6.765	.066	16	6.745	.121	6.582	.192

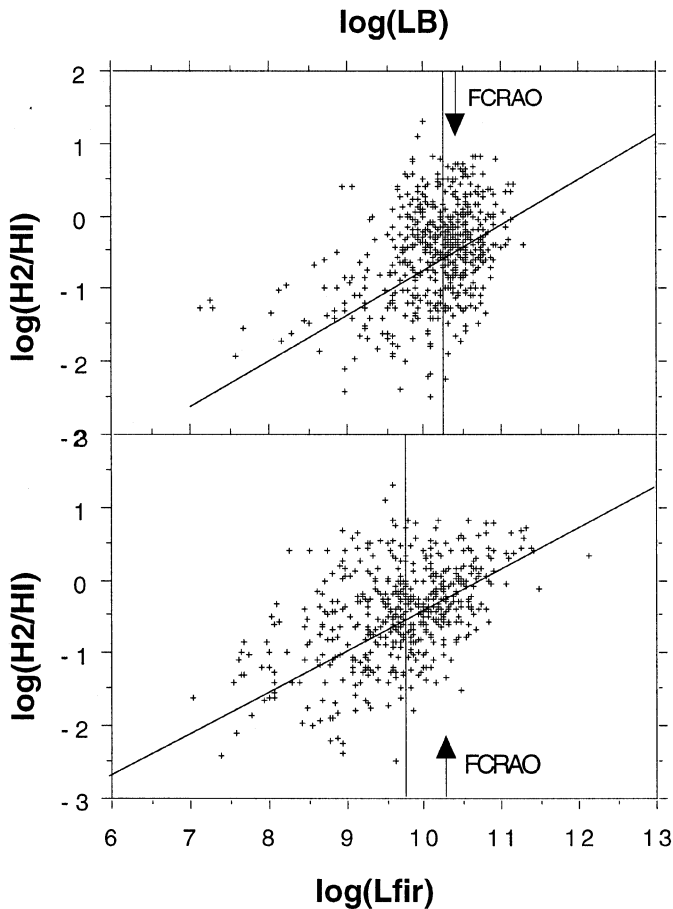


**Fig. 3a and b.** Variation of the molecular fraction  $M_{\text{H}_2}^i/M_{\text{HI}}$  with blue **a** and far-infrared **b** luminosities. The median values of  $L_B$  and  $L_{\text{FIR}}$  for the FCRAO extragalactic survey (Young et al. 1995) are indicated.

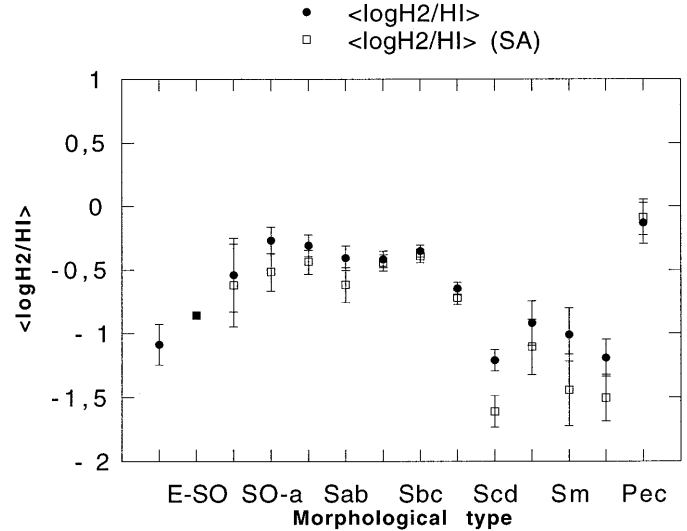


**Fig. 4.** Variation of the molecular fraction  $M_{\text{H}_2}^i/M_{\text{HI}}$  along the morphological type sequence. The dots show mean values with upper limits treated as detections, while the errorbars give the error on the mean. Open squares give the mean values when upper limits are taken into account using the survival analysis method.

surprising since  $D_{25}$  and  $M_{\text{dyn}}$  show different dependences on morphological type (see e.g. Roberts & Haynes 1994).

We have also investigated the dependence of the normalized gas contents upon the presence of a bar. The LEDA database does not distinguish between the intermediate bar (SAB) and barred (SB) types; both are quoted as barred. We find no significant differences (at the 5% level) in the gas contents, whatever the normalization, between the barred and unbarred galaxies.

**Table 2.** Mean and median values of the  $M_{\text{H}_2}^i/M_{\text{HI}}$  ratio, for different groups of morphological types

T	N/Nd	$\langle \rangle$	s.e.	$\langle \rangle_{SA}$	s.e.	med	s.e.
E	3/3	-1.086	0.160				
E-SO	1/1	-0.856					
S0	9/7	-0.542	.291	-0.622		-0.856	
S0-a	32/20	-0.268	.105	-0.517	0.149	-0.588	.235
Sa	39/28	-0.308	.083	-0.437	0.095	-0.504	.263
Sab	36/24	-0.408	.096	-0.618	0.137	-0.432	.173
Sb	77/68	-0.417	.064	-0.444	0.065	-0.475	.113
Sbc	101/88	-0.351	.047	-0.390	0.052	-0.369	.040
Sc	133/114	-0.647	.048	-0.717	0.057	-0.594	.039
Scd	27/11	-1.210	.084	-1.611	0.123	-1.616	.167
Sd	14/9	-0.918	.173	-1.105	0.216	-1.408	.376
Sm	14/6	-1.009	.209	-1.441	0.280	-2.171	.590
Irr	22/12	-1.191	.145	-1.503	0.182	-1.696	.321
Pec	16/13	-0.132	.163	-0.085	0.141	0.025	.335

Although we are not on very firm grounds, since whether a galaxy is classified as barred or unbarred will depend strongly on the image quality and on the galaxy distance, it is clear that any difference between barred and unbarred galaxies in their global CO(1–0) emission must be small.

### 3.2. The $M_{\text{H}_2}/M_{\text{HI}}$ ratio in disc galaxies

We now try to evaluate the relative importance of the molecular and atomic phases. In the HI-normal sample the mean value of  $\log(M_{\text{H}_2}^i/M_{\text{HI}}) = \log(0.20) \pm 0.04$ ; the median value is  $\log(0.27) \pm 0.06$  (errors are standard errors on the mean; survival analysis using the Kaplan-Meier estimator). These values become  $\log(M_{\text{H}_2}^i/M_{\text{HI}}) = \log(0.28) \pm 0.03$ , and  $\log(0.34) \pm 0.04$  if we consider only “classical” spirals (Sa to Sc’s). This also excludes most of the low-luminosity spirals, which are mainly late-type objects (see next Section).

Galaxies like M51, with  $(M_{\text{H}_2}^i/M_{\text{HI}}) = 3.5$ , seem then to be rare in the nearby universe. Many well-known grand-design spirals, such as M31 and M81, are indeed not especially  $\text{H}_2$ -rich, and this is also the case for the Milky Way: if we use the data of Bronfman et al. (1988) for the disc and those of Sanders et al. (1984) for the galactic center, we can estimate the total molecular mass in the Galaxy as  $M(\text{H}_2) = 1.2 \cdot 10^9 M_{\odot}$  while the atomic gas is about four times more abundant, with  $4.8 \cdot 10^9 M_{\odot}$  of HI (Henderson et al. 1982) (these figures are given for a solar galactocentric radius of 10 kpc). However, one should note that in our Galaxy as well as in others, the radial distributions of the two components are different (see Sect. 6.2).

We have investigated the relationship between the molecular gas fraction  $M_{\text{H}_2}^i/M_{\text{HI}}$  and various quantities and found that the correlations with  $M_{\text{dyn}}$ ,  $L_{\text{B}}$ ,  $\sigma_{\text{FIR}}$  and  $L_{\text{FIR}}$  were significant, that with  $L_{\text{FIR}}$  being the most significant one. This shows that large galaxies have more gas in molecular form; and that, if we can directly relate FIR luminosity to star formation, a higher

molecular fraction favors star formation activity. Fig. 3 shows the relation between the molecular fraction  $M_{\text{H}_2}^i/M_{\text{HI}}$  and the blue and far-infrared luminosities. Both correlations have less than  $10^{-4}$  probability to happen by chance. However, for a given value of  $L_{\text{FIR}}$  and  $L_{\text{B}}$ ,  $M_{\text{H}_2}^i/M_{\text{HI}}$  is spread by more than one order of magnitude.

### 3.3. Molecular fraction, morphological types and dynamical masses

The molecular gas fraction,  $M_{\text{H}_2}^i/M_{\text{HI}}$ , shows also a variation with morphological types (Fig. 4 and Table 1). Between Sa and Sc, the ratio is almost constant and shows a marked decrease from Scd to Irr. This is different from S93, who found a continuous decrease from early to late-types, of about a factor of ten, and also from YK, who found the same kind of behavior with a much larger amplitude. We find that this trend can be attributed to both the atomic and the molecular phases, and not only to the increase in  $M_{\text{HI}}/D_{25}^2$  with type: there is indeed a slight decrease of  $M_{\text{H}_2}^i/D_{25}^2$  with type (Fig. 1).

For peculiar objects, the  $M_{\text{H}_2}^i/M_{\text{HI}}$  ratio is close to unity. This is not unexpected since most of these objects have been chosen for their FIR emission. The same selection effect could be responsible for the relatively high  $M_{\text{H}_2}^i/M_{\text{HI}}$  ratio observed for S0-a.

Following a suggestion of the referee, we have investigated whether the behavior of the  $M_{\text{H}_2}^i/M_{\text{HI}}$  ratio with morphological types depends upon the dynamical mass of the galaxy. An estimate of  $M_{\text{dyn}}$  is available for 399 sample galaxies. We have used the same mass classes as in S93 (defined in Table 3): mI corresponds to the highest mass galaxies (about half of the sample), while mII to mV are lower mass objects. The variation of  $M_{\text{H}_2}^i/M_{\text{HI}}$  with morphological types split by mass classes is shown in Fig. 5.

The four lowest dynamical mass bins show the same trend as the whole sample: the molecular fraction decreases for late-types, beginning at Sc’s. However, there is no such trend for the upper mass bin mI ( $M_{\text{dyn}} > 10^{11} M_{\odot}$ ) for which the  $M_{\text{H}_2}^i/M_{\text{HI}}$  ratio stays constant at a value of about 0.4. Could this effect arise from early-type objects being erroneously classified as late-type? This is unlikely for Sc’s, since there are 40 objects of this type in the mI class. As for Scd-Irr, there are only 7 mI galaxies in this type range; we have checked their classifications and they appear reliable. Finally, there is no reason that this would happen for mI galaxies only and not for the other mass classes.

This behavior could explain why the trend that we find for the whole sample is different from S93. Indeed, the distance-limited sample of S93 contains many dwarf galaxies that exhibit lower molecular fractions for late morphological types.

Most of this phenomenon can be attributed to the molecular phase. Indeed, Fig. 6 shows that while the global trend is of increasing  $\sigma_{\text{HI}}$  with type for all mass bins, for  $\sigma_{\text{H}_2}$  we see a constant or even increasing value for mI, then for all other mass bins the trend is of decreasing  $\sigma_{\text{H}_2}$  for late-types.

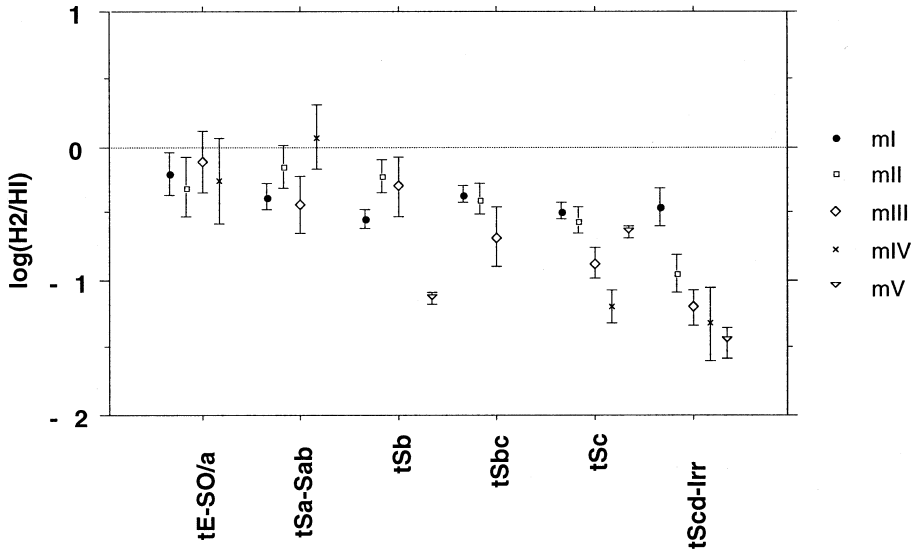


**Fig. 5.** Variation of the  $M_{H_2}^i/M_{HI}$  ratio along the morphological type sequence, split by dynamical mass. For galaxies in the upper dynamical mass class (mI, with  $M_{dyn} > 10^{11} M_{\odot}$ ), there is no trend of decreasing molecular fraction for late-type objects.

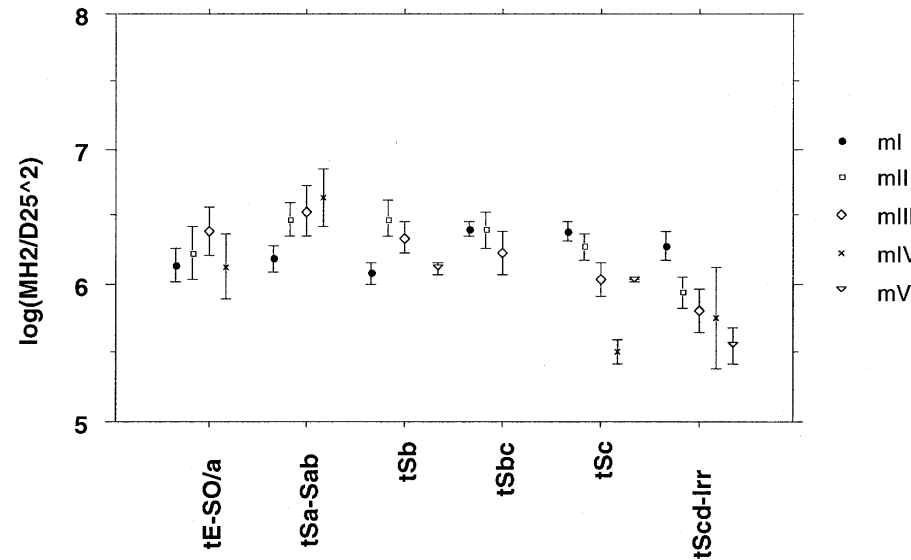
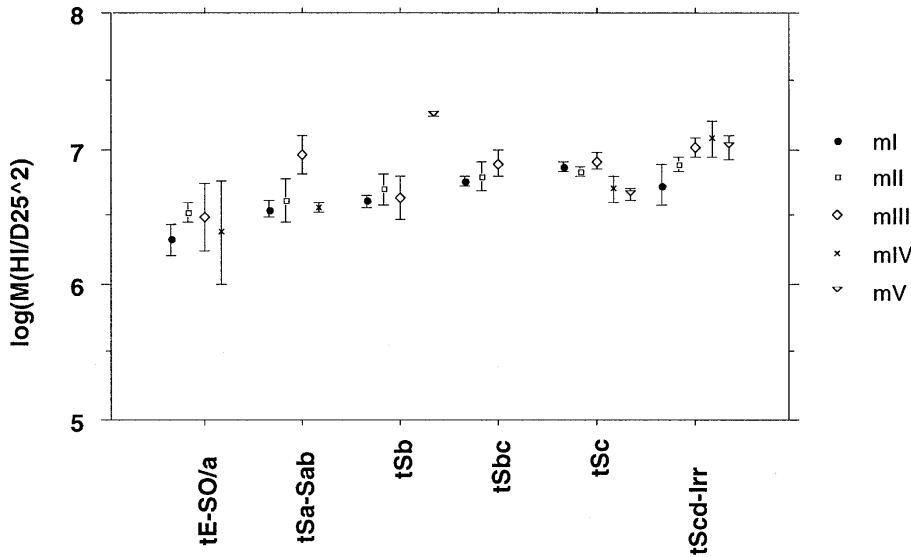


**Fig. 6.** Variation of the gas surface densities along the morphological type sequence, split by dynamical mass. For  $\sigma_{HI}$ , there is no difference between the mass classes. For  $\sigma_{H_2}$ , the trend is of increasing values for late-types in the upper mass bin, and the reverse for the lowest ones.

**Table 3.** Definition of the dynamical mass classes

Class	Mass range	Number
mI	$M > 10^{11} M_{\odot}$	195
mII	$5 \cdot 10^{10} M_{\odot} < M < 10^{11} M_{\odot}$	90
mIII	$1 \cdot 10^{10} M_{\odot} < M < 5 \cdot 10^{10} M_{\odot}$	77
mIV	$5 \cdot 10^9 M_{\odot} < M < 1 \cdot 10^{10} M_{\odot}$	18
mV	$M < 5 \cdot 10^9 M_{\odot}$	19

#### 4. The CO(1–0) emission of isolated and cluster galaxies

##### 4.1. The CO(1–0) emission of isolated galaxies: a predictor

We now try to identify the relevant parameters which would allow to predict the CO(1–0) emission/molecular content of spirals. In order to study the effect of environment on the molecular gas content of galaxies, we have first to define and study a comparison subsample of isolated galaxies. To this purpose, we will use the isolated galaxies (labelled as ISOL), but since there are only 105 ISOL objects with HI and CO data, we will also include galaxies belonging to peripheral regions of clusters. Cluster galaxies have then been separated in two categories, CENTER and OUTSKIRTS, in a way that depends upon which cluster was considered. For Coma and A1367, we have used the aggregation parameter *Agg* (Gavazzi 1987): for *Agg* = 1, 2, 3 or 4, the galaxies are considered as CENTER, while they are OUTSKIRTS for the other values of *Agg*. For Fornax and Virgo, whether a galaxy is CENTER or OUTSKIRTS depends upon its distance to the cluster center. The limit between the two regions has been varied from 3° to 5°, with no significant differences. In the following, this limit will be kept at 5°. There are then 105 galaxies in the ISOL subsample (82 detected in CO(1–0)) and 102 in the OUTSKIRTS one (81 detected), so that our reference sample amounts to 225 objects.

What are then the relevant parameters? It is clear that “size” and “form”, which have a very good predicting power for HI (HG), are not sufficient for CO(1–0). This can be suspected from inspection of Table 1: standard errors are systematically higher for  $H_2$  than for HI. A third parameter seems therefore necessary. As it is widely known that the far-infrared luminosity is a good predictor of the CO brightness of a galaxy, we have investigated  $L_{\text{FIR}}$  and  $L_{\text{FIR}}/D_{25}^2$  as the third parameter, but also, as a check, the blue luminosity  $L_B$  and the blue surface brightness  $L_B/D_{25}^2$  (we have also investigated the relationships with dynamical mass, but we have found that it is of much lower importance than  $L_{\text{FIR}}$  and  $L_{\text{FIR}}/D_{25}^2$ ).

Fig. 7 presents the variations of  $M_{\text{H}_2}^i/D_{25}^2$  and  $M_{\text{HI}}/D_{25}^2$  with the blue luminosity and the blue surface brightness. Fig. 8 presents the variations of the same quantities with the FIR luminosity and the FIR surface brightness. As was already found by HG84,  $M_{\text{HI}}/D_{25}^2$  is almost independent of  $L_B$  and very weakly dependent on  $L_B/D_{25}^2$  (this is why they chose  $M_{\text{HI}}/D_{25}^2$  as the best predictor of the HI content). It is also independent of the FIR emission, which is a nice and expected behavior.

As for the molecular gas content, it shows a strong and significant variation with both the blue surface brightness and FIR

**Table 4.** Values of the a(T) and b(T) coefficients, used to compute the expected value of the molecular content  $\log((M_{\text{H}_2}^i/D_{25}^2)_e)$ , from linear regressions of the form  $\log(M_{\text{H}_2}^i/D_{25}^2)_e = a(T) \log(L_{\text{FIR}}/D_{25}^2) + b(T)$ . a(T) and b(T) are given for each morphological type bin. Survival analysis was used. Peculiar galaxies are not included in the sample, which contains only the ISOL and OUTSKIRTS categories (see text).

T	N	a(T)	s.e.	b(T)	s.e.
E-SO/a	9	0.54	0.33	2.21	2.30
Sa-Sab	27	0.60	0.14	1.87	1.00
Sb	36	0.61	0.16	1.90	1.05
Sbc	40	0.75	0.10	1.04	0.74
Sc	54	0.74	0.10	0.94	0.70
Scd-Irr	20	0.80	0.10	0.40	0.72
All	187	0.71	0.05	1.17	0.37

luminosity, and an even stronger one with the far-infrared surface brightness  $\sigma_{\text{FIR}}$ . It is thus important to take the latter variation into account if one wants to predict the CO(1–0) emission of a galaxy with some accuracy, or to compare different samples.

We have found in the previous Section that there is a dependence of  $M_{\text{H}_2}^i/D_{25}^2$  with morphological type. Part of it is likely due to the dependence of  $\sigma_{\text{FIR}}$  with type, which follows roughly the same pattern (see also Roberts & Haynes 1994).

We can then define an “expected” value of the normalized molecular hydrogen mass,  $(M_{\text{H}_2}^i/D_{25}^2)_e$ , using linear regressions:  $\log((M_{\text{H}_2}^i/D_{25}^2)_e) = a(T) \log(L_{\text{FIR}}/D_{25}^2) + b(T)$ . T is the morphological type of the galaxy, or a group of morphological types (e.g. Scd-Irr), chosen in the same way as HG84. The values of a(T) and b(T) are given in Table 4.

##### 4.2. The effect of environment on the CO(1–0) emission of galaxies

Now that we have a way to estimate the expected CO(1–0) emission of an “isolated” galaxy, we can try to evaluate the effects of the galaxy environment on their CO(1–0) emission/molecular gas content. To this aim, we define a CO deficiency parameter, CODEF, and another one, ENV, which describes the galaxy environment.

ENV contains four categories: ISOL, OUTSKIRTS, CENTER, and INTER. ISOL and OUTSKIRTS galaxies have been defined in the previous section. For cluster galaxies, we now have the CENTER category: all cluster objects that do not fall in the OUTSKIRTS category. The fourth group, INTER, gathers 23 galaxies which are known to be strongly interacting, such as ring galaxies (Horellou et al. 1995b). As a check, we have also computed the values of the HI deficiency HIDEF.

CODEF is computed using the results of the previous Section, in the following way:

$$\text{CODEF} = \log(M_{\text{H}_2}^i/D_{25}^2)_e - \log(M_{\text{H}_2}^i/D_{25}^2)_{\text{obs}},$$

where  $(M_{\text{H}_2}^i/D_{25}^2)_{\text{obs}}$  and  $(M_{\text{H}_2}^i/D_{25}^2)_e$  are respectively the observed and expected value of this parameter. With this definition, CODEF is positive when the galaxy is deficient in CO emission. Pec galaxies have not been considered in the previous Section;

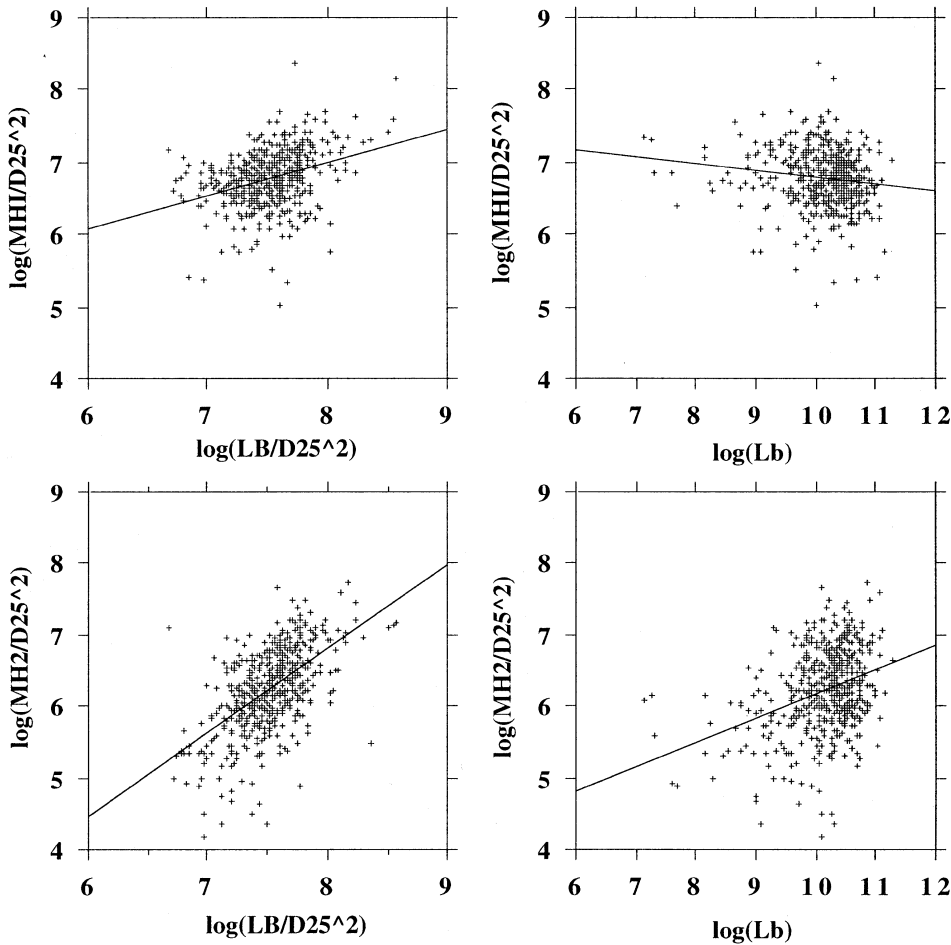


**Fig. 7.** Variation of the normalized gas masses  $M_{\text{H}_2}^1/D_{25}^2$  and  $M_{\text{HI}}/D_{25}^2$  with the blue luminosity  $L_B$  and the blue surface brightness  $L_B/D_{25}^2$ . There is little variation for the atomic phase and a significant one for the molecular phase.

**Table 5.** Mean values of the CO deficiency, CODEF, and of the HI deficiency, HIDEF, for different galaxy environments ENV. CENTER galaxies are those belonging to cluster cores, OUTSKIRTS are found in the outer parts of clusters, ISOL are galaxies from the Karachenseva catalog, while INTER are interacting galaxies such as rings.

ENV	N	<CODEF>	s.e.	<HIDEF>	s.e.
CENTER	67	0.107	0.055	0.558	0.055
OUTSKIRTS	82	0.015	0.031	0.012	0.046
ISOL	105	-0.011	0.033	-0.030	0.031
INTER	23	0.046	0.072	0.047	0.103

we will compare their CO emission with that of the reference sample described before, with no distinction of morphological type (last line in Table 4.1).

Mean values of CODEF and HIDEF are given in Table 4.2, while the probabilities that there are significant differences between the sub-samples are given in Table 6. As expected, CENTER galaxies are significantly HI-deficient, while OUTSKIRTS have the same mean (null) deficiencies than ISOLATED within the errors (this justifies the use of OUTSKIRTS galaxies as a reference sample for CENTER objects, see Sect. 4). On the other hand, we find *no significant difference* at the 5% percent level between any subsamples for their CO deficiency.

**Table 6.** Probabilities that galaxies in different environments have the same mean value of the CO deficiency (column 2) and HI deficiency (column 3). These mean values are given in Table 6. As expected, galaxies in cluster cores and outer regions have significantly different HI contents, core galaxies being HI-deficient and the others not. On the other hand, there is no significant variation of the CO deficiency with the galaxy environment, the mean value of CODEF being always consistent with 0.

(ENV1, ENV2)	P(CODEF)	P(HIDEF)
CENTER, OUTSKIRTS	0.18	<0.0001
CENTER, ISOL	0.32	<0.0001
CENTER, INTER	0.80	<0.0001
OUTSKIRTS, ISOL	0.60	0.43
OUTSKIRTS, INTER	0.12	0.74
ISOL, INTER	0.25	0.36

We then conclude that in this sample, we see no sign of a modification in any sense of the CO emission of galaxies in the core of the Virgo, Fornax, Coma and A1367. This establishes on firmer grounds the conclusions drawn by Kenney & Young (1989) for the Virgo cluster, for the Coma supercluster by Casoli et al. (1991), and for the Fornax cluster by Horellou et al (1995b), which were all given in the absence of a reference sample.

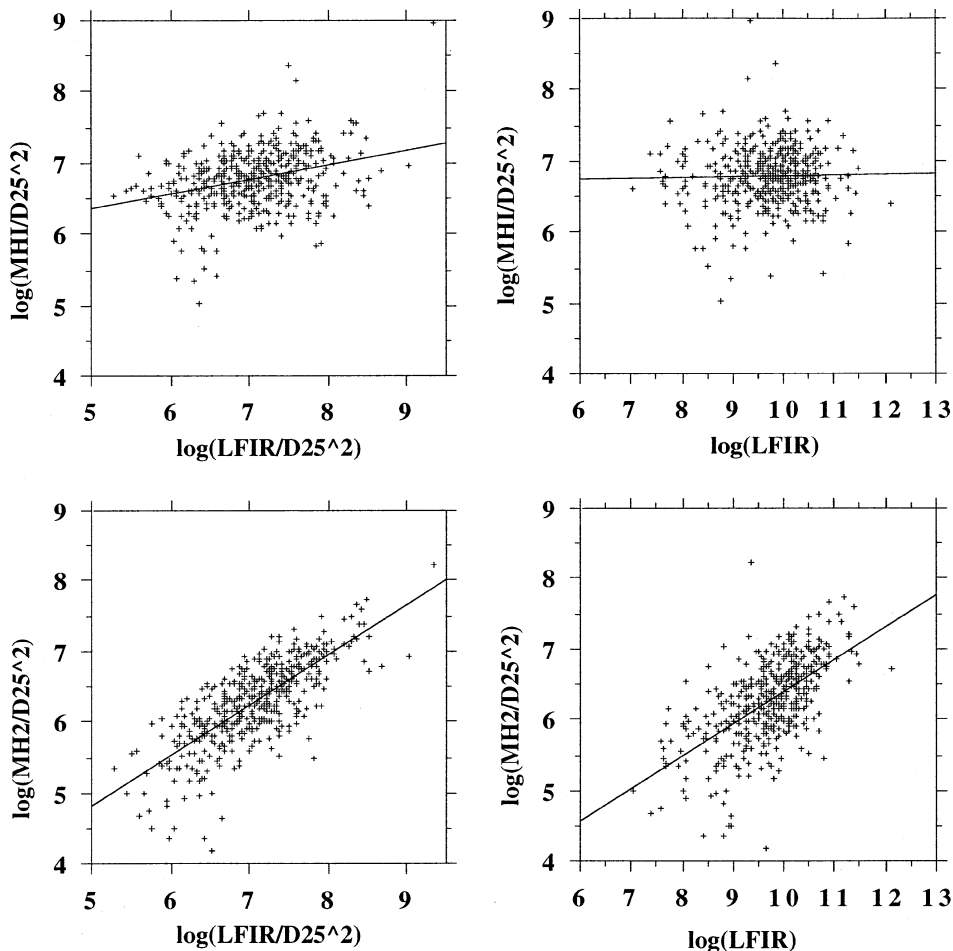


**Fig. 8.** Variation of the normalized gas masses  $M_{\text{H}_2}^i/D_{25}^2$  and  $M_{\text{HI}}/D_{25}^2$  with the far-infrared luminosity  $L_{\text{FIR}}$  and the far-infrared surface brightness  $L_{\text{FIR}}/D_{25}^2$ . There is little variation for the atomic phase, but a strong one for the molecular component.

As for the interacting galaxies in our sample, they do not seem especially rich in  $\text{H}_2$ . This may seem in contradiction with the current wisdom that interacting galaxies are FIR-bright, and that FIR-bright galaxies are CO-bright. However, our definition of the normal CO emission/ $\text{H}_2$  content of a galaxy includes the far-infrared surface-brightness as a parameter. Moreover, interacting galaxies are not all FIR-bright, though the reverse may be true. CO surveys of optically-selected interacting galaxies have found that they have a low CO emission, that is, undetectable in many cases (Horellou & Booth, 1997), and Solomon & Sage (1988) have found that high  $\text{H}_2$  mass galaxies are not all interacting. It is mainly the far-infrared emission that governs the CO emission, and not the presence of an interaction.

### 5. Far-infrared emission, molecular gas and morphological type

The ratio between the far-infrared luminosity and the molecular gas mass,  $L_{\text{FIR}}/M_{\text{H}_2}^i$ , has often been presented as a measure of the massive-star formation efficiency. There is some debate about this point, since it seems that a non-negligible, but not well determined, fraction of the far-infrared emission is not directly due to ionizing stars (e.g. Devereux & Young 1991, Young et al. 1996, Sauvage & Thuan 1992, Calzetti et al. 1995, Buat &

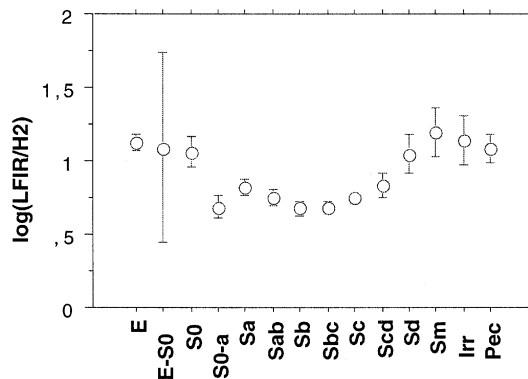


**Fig. 9.** Variations of the  $L_{\text{FIR}}/M_{\text{H}_2}^i$  ratio along the morphological type sequence.

Xu 1996). We will not enter into this debate here, but examine whether we find a variation of  $L_{\text{FIR}}/M_{\text{H}_2}^i$  with morphological type. Fig. 9 shows this variation. We find that late-type galaxies have higher values of  $L_{\text{FIR}}/M_{\text{H}_2}^i$ . This increase amounts to a factor of about 3 (this effect is significant: in Fig. 9, errors bars are  $1\sigma$  errors). This is at variance to previous claims by Devereux & Young (1991).

## 6. Discussion

### 6.1. Comparison with previous results

Our finding that there is much more HI than H<sub>2</sub> in disc galaxies confirms on a much larger sample the previous results of S93, Horellou et al. (1995b), Casoli et al. 1996, and Boselli et al. (1997), but stands in strong contrast with that of YK. Apart from a slight difference in the X factor, since YK adopted a value of  $2.8 \cdot 10^{20} \text{ cm}^{-2} / (\text{K kms}^{-1})$ , we see several reasons for this discrepancy. First, while our complete sample contains most of the YK one, since it contains the whole FCRAO survey (with the exception of the objects observed by Sage 1993a), we have excluded very HI-deficient objects. Conversely, the YK sample contains many HI-deficient objects belonging to the Virgo cluster. This can explain part of the discrepancy for the mean ratio, as well as the morphological type variation, since it appears that early-type objects are most affected by the HI-deficiency.

A part of the difference could also be related to the way the statistical analysis is made. Because of the wide range of the  $M_{\text{H}_2}^i / M_{\text{HI}}$  ratios, we have chosen to compute the mean of the logarithms of this ratio, which is different from (and lower than) the logarithm of the mean. There is of course no difference for the medians. In addition, using survival analysis decreases the molecular gas fraction, since about one-fourth of the galaxies are not detected in CO(1–0). Finally, the fact that the FCRAO sample contains mostly FIR and optically bright objects could also be an explanation since it leads to observing CO-bright objects. In Figs. 7 and 8, the median values of  $L_{\text{B}}$  and  $L_{\text{FIR}}$  for the FCRAO sample are indicated as arrows, and are clearly located in the region where high values of  $M_{\text{H}_2}^i / M_{\text{HI}}$  are found. All these differences go in the same direction, and it is thus not surprising that we find lower values for the molecular gas contents.

### 6.2. Molecular gas fraction in the star-forming disc

Our previous discussion concerns galaxies as a whole. Our results do not imply that in the star-forming disc, HI is also predominant, because it is well known that H<sub>2</sub> is found in the *inner* regions and HI in the *outer* regions of galaxies (e.g. Sofue 1997, Sage & Solomon 1991). For most of the sample galaxies there is no information on the actual distribution of the CO and HI emissions; we have then tried to take this into account in a statistical way. We have used the data from Warmels (1986) to estimate the ratio between the total HI mass and the HI mass inside half of the 25-th magnitude radius (this is roughly the overall extent of the CO emission, Young et al. 1995). For a sample of 57 Sa-Sd galaxies, the median value of this ratio is 2.1, that is, half of the HI mass is found inside  $R_{25}/2$ . Within this radius, the  $M_{\text{H}_2}^i / M_{\text{HI}}$  ratio is then between 40 and 70 percent.

Another way to estimate this fraction is to consider the *HI-deficient galaxies* only. Indeed, observations suggest that moderately deficient objects have been stripped of their atomic gas in the outer regions, but that their inner gas is not affected. Very deficient galaxies should however be HI-deficient even in their central regions: this is the result found by Cayatte et al. (1994)

for Virgo galaxies. From their data, it seems that the borderline between galaxies which are affected over their whole disc and those which are not lies at an HI deficiency around 0.6. We have thus computed the  $M_{\text{H}_2}^i / M_{\text{HI}}$  ratio for galaxies with  $0.3 < \text{HIdef} < 0.6$ . There are 27 such galaxies, all of morphological type between Sa and Sc (as Cayatte et al. remark, late-type deficient objects are rare), 21 are detected in CO(1–0), and the mean value of  $M_{\text{H}_2}^i / M_{\text{HI}}$  is  $61 \pm 10$  percent. Although this estimate is a very rough one, it gives the same order of magnitude as the previous one.

### 6.3. Variations of the conversion factor X

Our conclusions are clearly dependent on the actual value of the conversion factor for each galaxy. In classical spirals, there are several indications that the conversion factor between CO(1–0) emissivities and H<sub>2</sub> masses could be lower than our adopted value of  $2.3 \cdot 10^{20}$ . For our Galaxy, recent analysis of the Gamma-Ray Observatory data suggests a global value around  $1.5 \cdot 10^{20}$  (Digel et al. 1996). Other indications in the same direction come from observations of the continuum emission at 1mm of the central regions of NGC 891 and M51 by Guélin et al. (1993, 1995), and of the disk of NGC4565 by Neininger et al. (1996). This continuum emission traces the cold dust and, with an estimate of the dust temperature, allowed them to derive gas masses independently of the CO(1–0) observations. The molecular gas masses that they find are several times lower than deduced from the CO observations, which also points towards a low value of X. This would mean that the actual H<sub>2</sub> masses are even lower than what we find, and that the atomic phase is even more dominant.

The determination of X in late-type spirals and irregular galaxies is a difficult problem, because of the lack of independent determinations of the H<sub>2</sub> mass. For the Small Magellanic Cloud, Rubio et al. (1993) have suggested a high value of X, about  $9 \cdot 10^{20} \text{ cm}^{-2} / (\text{K kms}^{-1})$ , by assuming that the virial masses of the clouds are equal to their molecular masses. However these clouds may not be in equilibrium and may still contain a large amount of atomic hydrogen. The uncertainties are not so high that they can change our main conclusion, that there is more HI than H<sub>2</sub> in all types from SO's to Irr.

The fact that high-mass late-type spirals have a higher molecular fraction than low-mass ones (Sect. 3.3) could be attributed to a variation of X. Indeed, the standard conversion factor almost certainly underestimates the true molecular mass in objects with a low metallicity, a low dust content and a high radiation field, which could be the case for the CO-weak late-type objects. On the other hand, we have found no difference between the optical colors (U-B) and (B-V) of the high-mass and low-mass late-type objects; neither did we find a difference in their  $L_{\text{FIR}} / M_{\text{H}_2}$  ratio. Thus it seems that the difference between high-mass and low-mass late-type spirals is not due to a difference in X. One may speculate that massive galaxies form molecular clouds more easily through the effect of stronger density waves (see also Elmegreen 1993). The causes of their different behaviors remain to be explored.

#### 6.4. Some consequences of the low values of the molecular gas fraction

The low  $H_2$  content of spirals observed in this analysis raises an interesting question. With a median molecular gas content of  $1.3 \cdot 10^9 M_\odot$ , how will spiral galaxies (Sa-Sc) be able to sustain reasonably high star formation rates for more than a few billion years? If we compute roughly the molecular gas exhaustion time scale by estimating the star formation rate from the far-infrared luminosity using

$$\tau = M_{H_2}^i / (1.4 \cdot 10^{-10} L_{FIR}) \text{ (Sauvage \& Thuan 1992),}$$

(this does not take into account the return of gas to the interstellar medium, but we need only an order of magnitude), we find that half of the sample galaxies will have exhausted their molecular gas reservoir in less than  $1.3 \cdot 10^9$  yr. To escape this problem, we can envisage that there are actually large exchanges between the atomic and molecular phase. If all the atomic hydrogen inside  $R_{25}/2$  is converted eventually into molecular gas,  $\tau$  can be enhanced by a factor of 2. If this is not sufficient, the unescapable consequence is that there must be some inward motions of the atomic gas in order to refuel the inner regions. Such motions should be detectable by comparing the HI and CO(1–0) velocity fields in nearby spirals. This problem has been already raised by Blitz (1997) for the Milky Way, who reached similar conclusions.

If the atomic phase is more closely linked to the molecular one than usually thought of, it could also exhibit some link with the star formation tracers. Indeed, several authors (Buat 1992, Boselli 1994, Casoli et al. 1996, and references therein) have found good relationships between various star formation indicators and the HI content. This can be understood if the transformation of HI into  $H_2$  is a slow process (indeed Heck et al. 1992 estimate that the characteristic conversion time is larger than  $10^7$  yr), while the molecular phase is relatively short-lived, either because it forms stars or it is disrupted by star formation. The atomic phase would then be the limiting factor in the cycle HI -  $H_2$  - stars. Another interpretation has been proposed by Elmegreen (1993), in which the transition HI- $H_2$  is mainly governed by the external pressure and radiation field; if molecular clouds are not always self-gravitating, the molecular mass fraction in a galaxy could indeed be a poor indicator of its star-forming properties.

Finally let us point out that the fact that with present-day receivers and telescopes, the CO(1–0) emission of a normal spiral (that is, not especially selected for its far-infrared luminosity) is often undetectable at a redshift as small as a few thousand  $\text{km s}^{-1}$ . This suggests that even in deep surveys, the CO emission of the large majority of distant spiral galaxies will not be easily detectable.

## 7. Conclusions

The following conclusions have been reached in this study of a large sample of disc galaxies observed both in HI and CO(1–0) :

1. In the sample spiral galaxies, there is more HI than  $H_2$ , with only about one fourth to one third of the gas in molecular

form in Sa-Sc spirals. This still holds if one considers the star-forming disc only, which has an  $M_{H_2}^i/M_{HI}$  ratio of about sixty percent,

2. This value of the molecular gas fraction has been obtained from CO(1–0) observations using a conversion factor  $X = 2.3 \cdot 10^{20}$ . The previous conclusion is reinforced if, as suggested by recent  $\gamma$  ray and millimeter-wave continuum observations, the value of X for Sa-Sc spirals is actually lower,
3. We find a decrease of the molecular to atomic gas mass ratio for late-types, beginning at Scd's. This variation is due to the conjunction of two factors: the increase of the mass of gas in atomic form, and the decrease of the molecular gas amount. It is milder than what has been found in previous studies, late-type objects (Scd to Irr) having 1/10 of their gas in molecular form,
4. This decrease is actually related to the dynamical mass of the galaxy, and is absent for objects with  $M_{dyn} > 10^{11} M_\odot$ . The reasons for this difference remain to be explored,
5. We give a recipe to estimate the molecular gas content/CO(1–0) emission of a galaxy knowing its size ( $D_{25}^2$ ), form (morphological type), and far-infrared emission ( $L_{FIR}/D_{25}^2$ ). This allows us to define a CO deficiency parameter, CODEF, analogous to what has been defined for the HI emission. Using this parameter, we show that galaxies in cluster cores, which are strongly deficient in their HI emission, are not CO-deficient.

*Acknowledgements.* We gratefully thank the NRAO staff for its assistance during the remote observing sessions. We have used the SIMBAD database from the Centre de Données de Strasbourg (France) to retrieve bibliographic data, the Lyon-Meudon Extragalactic Database (LEDA) supplied by the LEDA team at the CRAL-Observatoire de Lyon (France), and of the NASA Extragalactic Database. We thank the referee, Leslie Sage, for useful suggestions.

## References

- Andreani P., Casoli F., Gerin M., 1995, A&A 300, 43  
 Blitz, L., 1997, in "CO: twenty-five years of millimeter-wave spectroscopy", IAU Symposium 170, eds W.B. Latter, S.J.E. Radford, P.R. Jewell, J.G. Mangum, J. Bally, Kluwer Academic Publishers, p. 11  
 Boselli A., 1994, A&A 292, 1  
 Boselli A., Gavazzi G., Combes F., Lequeux J., Casoli F., 1994, A&A 285, 69  
 Boselli A., Gavazzi G., Lequeux J. et al. 1995a, A&A 300, L13  
 Boselli A., Casoli F., Lequeux J., 1995b, A&AS 110, 521  
 Boselli A., Mendes de Olivera C., Balkowski C., Cayatte C., Casoli F., 1996, A&A 314, 738  
 Boselli A., Gavazzi G., Lequeux J., et al. 1997, submitted to A&A  
 Bronfman L., Cohen, R., Alvarez H., et al. 1988, ApJ 324, 248  
 Buat V., 1992, A&A 264, 44  
 Buat V., Xu C., 1996, A&A 306, 61  
 Calzetti D., Bohlin R., Kinney A., Storchi-Bergmann T., Heckman T., 1995, ApJ 443, 136  
 Casoli F., Boissé P., Combes F., Dupraz C., 1991, A&A 249, 359  
 Casoli F., Dickey J., Kazès I., et al. 1996, A&AS 116, 193  
 Cayatte V., Kotanyi C., Balkowski C., van Gorkom J. H., 1994, AJ 107, 1003

- Devereux N., Young J., 1991, *ApJ* 371, 515
- Digel S., Grenier I., Heithausen A., et al. 1996, *ApJ* 463, 604
- Elmegreen B.G., 1993, *ApJ* 411, 170
- Gavazzi G., 1987, *ApJ* 320, 96
- Gerin M., Casoli F., 1994, *A&A* 290, 49
- Giovanelli R. & Haynes M., 1985, *ApJ* 292, 404
- Guélin M., Zylka R., Mezger P.G., et al. 1993, *A&A* 279, L37
- Guélin M., Zylka R., Mezger P.G., et al. 1995, *A&A* 298, L29
- Haynes M. P., Giovanelli R., 1984, *AJ* 89, 758 (HG84)
- Heck E., Flower D., Le Bourlot J., Pineau des Forêts G., Roueff E., 1992, *MNRAS* 258, 377
- Henderson A., Jackson P., Kerr F., 1982, *ApJ* 263, 116
- Horellou C., Casoli F., Combes F., Dupraz C., 1995a, *A&A* 298, 743
- Horellou C., Casoli F., Dupraz C., 1995b, *A&A* 303, 361
- Horellou C., Booth R.S., 1997, to appear in *A&AS*
- Isobe T., Feigelson E., Nelson P.I., 1986, *ApJ* 306, 490
- Karachenseva V., 1973, *Comm. Spec. Astrophys.* 8
- Kenney J.D.P., Young J.S., 1989, *ApJ* 344, 171
- Lequeux J., 1996, in “The interplay between massive star formation and galaxy evolution”, 11th IAP meeting, éditions Frontières
- Neininger N., Guélin M., Garcia-Burillo S., et al. 1996, *A&A* 310, 725
- Roberts M.S., Haynes M.P., 1994, *ARA&A* 32, 115
- Rubio M., Lequeux J., Boulanger F., 1993, *A&A* 271, 9
- Sage L. J., 1993a, *A&A* 272, 123 (S93)
- Sage L. J., 1993b, *A&AS* 100, 537
- Sage, L.J., Solomon, P.M., 1991, *ApJ* 380, 392
- Sanders D.B., Solomon P.M., Scoville N.Z., 1984, *ApJ* 276, 182
- Sauty S., Casoli F., Boselli A., et al, 1997, submitted to *A&AS*
- Sauvage M., Thuan T.X., 1992, *ApJ* 396, L69
- Sofue, Y., 1997, in “CO: twenty-five years of millimeter-wave spectroscopy”, IAU Symposium 170, eds W.B. Latter, S.J.E. Radford, P.R. Jewell, J.G. Mangum, J. Bally, Kluwer Academic Publishers, p. 273
- Solomon P., Sage, L. J., 1988, *ApJ* 334, 613
- Strong A.W., Bloemen J.B.G.M., Dame T.M., et al. 1988, *A&A* 207, 1
- Warmels R.H., 1986, PhD Thesis, Groningen University
- Young J., Knezek P., 1989, *ApJ* 345, L55 (YK)
- Young J., Xie Shuding, Kenney, J. D. P, Rice, W. L., 1989, *ApJS* 70, 699
- Young J., Xie Shuding, Tacconi, L., et al. 1995, *ApJS* 98, 219
- Young J., Allen L., Kenney J.D.P., Lesser A., Rownd B., 1996, *AJ*, 112, 1903

This article was processed by the author using Springer-Verlag L<sup>A</sup>T<sub>E</sub>X A&A style file L-AA version 3.